The histone H2A deubiquitinase Usp16 regulates hematopoiesis and hematopoietic stem cell function

Yue Gu[a,1], Amanda E. Jones[a,1], Wei Yang[a,1], Shanrun Liu[a], Qian Dai[b], Yudong Liu[c], C. Scott Swindle[d], Dewang Zhou[a], Zhuo Zhang[a], Thomas M. Ryan[a], Tim M. Townes[a], Christopher A. Klug[d], Dongquan Chen[e], and Hengbin Wang[a,2]

[a]Department of Biochemistry and Molecular Genetics, Stem Cell Institute, University of Alabama at Birmingham, Birmingham, AL 35294; [b]Department of Pathology, University of Alabama at Birmingham, Birmingham, AL 35294; [c]Department of Cell, Developmental, and Integrative Biology, University of Alabama at Birmingham, Birmingham, AL 35294; [d]Department of Microbiology, University of Alabama at Birmingham, Birmingham, AL 35294; and [e]Division of Preventive Medicine, Comprehensive Cancer Center, University of Alabama at Birmingham, Birmingham, AL 35294

Edited by Louise T. Chow, University of Alabama at Birmingham, Birmingham, AL, and approved November 23, 2015 (received for review August 26, 2015)

Epigenetic mechanisms play important regulatory roles in hematopoiesis and hematopoietic stem cell (HSC) function. Subunits of polycomb repressive complex 1 (PRC1), the major histone H2A ubiquitin ligase, are critical for both normal and pathological hematopoiesis; however, it is unclear which of the several counteracting H2A deubiquitinases functions along with PRC1 to control H2A ubiquitination (ubH2A) level and regulates hematopoiesis in vivo. Here we investigated the function of Usp16 in mouse hematopoiesis. Conditional deletion of *Usp16* in bone marrow resulted in a significant increase of global ubH2A level and lethality. *Usp16* deletion did not change HSC number but was associated with a dramatic reduction of mature and progenitor cell populations, revealing a role in governing HSC lineage commitment. ChIP- and RNA-sequencing studies in HSC and progenitor cells revealed that Usp16 bound to many important hematopoietic regulators and that *Usp16* deletion altered the expression of genes in transcription/chromosome organization, immune response, hematopoietic/lymphoid organ development, and myeloid/leukocyte differentiation. The altered gene expression was partly rescued by knockdown of PRC1 subunits, suggesting that Usp16 and PRC1 counterbalance each other to regulate cellular ubH2A level and gene expression in the hematopoietic system. We further discovered that knocking down *Cdkn1a* (*p21cip1*), a Usp16 target and regulated gene, rescued the altered cell cycle profile and differentiation defect of *Usp16*-deleted HSCs. Collectively, these studies identified Usp16 as one of the histone H2A deubiquitinases, which coordinates with the H2A ubiquitin ligase PRC1 to regulate hematopoiesis, and revealed cell cycle regulation by Usp16 as key for HSC differentiation.

Usp16 | H2A deubiquitination | polycomb repressive complex 1 | hematopoiesis | hematopoietic stem cell

Hematopoiesis, where hematopoietic stem cells (HSCs) undergo sequential lineage commitment to generate all cell types in the blood, is controlled by an interactive network of transcription factors and epigenetic regulators (1–3). Polycomb group (PcG) proteins represent an important group of epigenetic regulators that contribute to the maintenance of cell-type–specific gene expression by repressing alternative gene expression programs (4–6). PcG proteins form multisubunit protein complexes to achieve gene repression function; for example, polycomb repressive complex 1 (PRC1) is composed of PcG proteins Bmi1, Cbx, Phc, and Ring1A/1B (7). PRC1 represses gene expression, at least in part, through histone H2A ubiquitination (ubH2A) (8, 9). Ring1A/1B is the catalytic subunit for PRC1-mediated H2A ubiquitination, whereas Bim1 is the scaffold for assembling the ubiquitin ligase complex (8, 10–12). It is proposed that ubH2A blocks RNA polymerase II elongation and serves as a final licensing factor for productive transcription (13, 14). Subunits of PRC1 are critical for both normal and pathological hematopoiesis (15–17). *Bmi1* knockout in mice reduces progenitor cell proliferation and causes hypo-cellular bone marrow (BM) (18). Hematopoietic cells in *Bmi1* knockout mice are also impaired in proliferative response to mitogens. The critical role of Bmi1 is largely attributed to dysregulation of the *Ink4A* locus (19). Bmi1 also plays an indispensable role in the maintenance of leukemic stem cells (19, 20). Furthermore, *Ring1B* knockout results in hypo-cellular BM but enlarged pools of hyper-proliferating immature cells. Although HSCs and progenitor cells maintain differentiation potential, they exhibit high proliferation rates (21). These alterations have been attributed to a differential regulation of cyclin D2, which is elevated in all mutant BM cells, and of p16 Ink4a, which is increased only in more differentiated compartments (21).

The steady level of cellular ubH2A is governed by the balance between the opposing enzymatic activities that add and remove the ubiquitin moiety. There are at least seven reported H2A deubiquitinases: USP3, USP12, USP16, USP21, USP22, USP46, and Mysm1 (22). *Usp3* and *Mysm1* knockout mice are viable, although both exhibit morphologic and functional abnormalities (23–25). *Mysm1* knockout mice are also born at lower-than-expected Mendelian ratios, but global ubH2A level is unchanged (23). Usp3 appears to regulate ubH2A and ubiquitinated H2B (ubH2B) levels in the context of DNA damage (25, 26). In contrast, biochemical and genome-wide ChIP-sequencing (ChIP-seq) studies revealed that Usp16 regulates ubH2A levels in human HeLa cells,

Significance

Polycomb repressive complex 1 (PRC1) represents an important epigenetic regulator, which exerts its effect on gene expression via histone H2A ubiquitination (ubH2A). We developed a conditional *Usp16* knockout mouse model and demonstrated that *Usp16* is indispensable for hematopoiesis and hematopoietic stem cell (HSC) lineage commitment. We identified Usp16 to be a H2A deubiquitinase that counterbalances the PRC1 ubiquitin ligase to control ubH2A level in the hematopoietic system. Conditional *Usp16* deletion led to altered expression of many regulators of chromatin organization and hematopoiesis. In addition, Usp16 maintains normal HSC cell cycle status via repressing the expression of *Cdkn1a*, which encodes p21cip1, an inhibitor of cell cycle entry. This study provides novel insights into the epigenetic mechanism that regulates hematopoiesis and HSC function.

Author contributions: H.W. designed research; Y.G., W.Y., S.L., Q.D., Y.L., C.S.S., and Z.Z. performed research; D.Z. contributed new reagents/analytic tools; Y.G., A.E.J., W.Y., S.L., Q.D., T.M.R., T.M.T., C.A.K., D.C., and H.W. analyzed data; and T.M.R., T.M.T., C.A.K., and H.W. wrote the paper.

The authors declare no conflict of interest.

This article is a PNAS Direct Submission.

Data deposition: High-throughput sequencing data reported in this paper have been deposited in the Gene Expression Omnibus (accession no. GSE62825).

[1]Y.G., A.E.J., and W.Y. contributed equally to this work.

[2]To whom correspondence should be addressed. Email: hbwang@uab.edu.

This article contains supporting information online at www.pnas.org/lookup/suppl/doi:10.1073/pnas.1517041113/-/DCSupplemental.

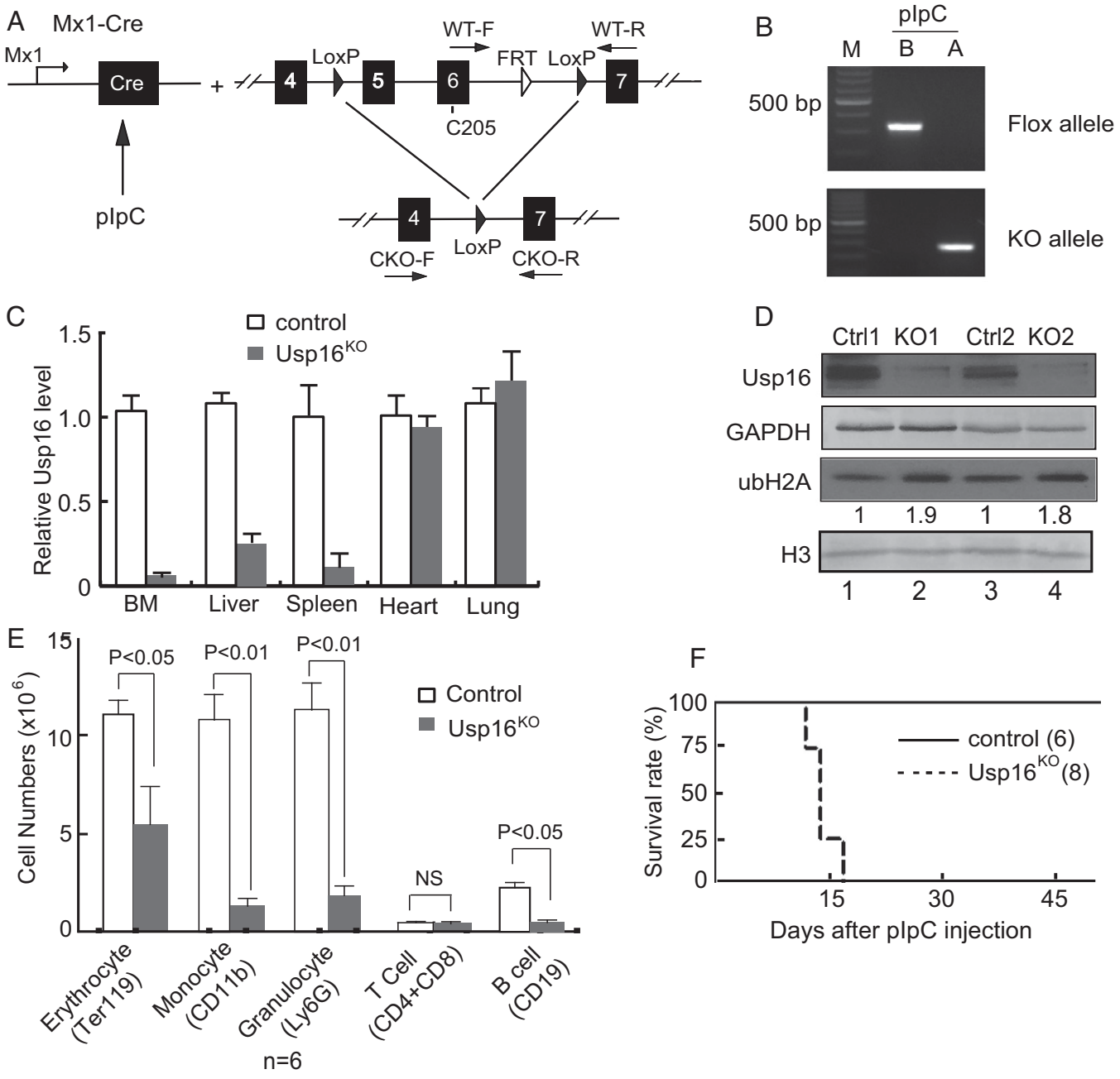

Fig. 1. *Usp16* regulates mouse hematopoiesis. (*A*) Schematic representation of the strategy used to delete *Usp16* in mouse hematopoietic system. The C205 residue required for the catalytic activity is indicated. (*B*) Images of PCR-mediated genotyping of *Usp16* in BM before (*B*) and after (*A*) pIpC injection. Primer pairs used to detect the predeleted allele and KO allele are shown in *A*. The primers for the KO allele could not amplify the long predeleted allele due to the PCR conditions. (*C*) RT-qPCR assay of *Usp16* transcript levels in selective tissues or organs of control and $Usp16^{KO}$ mice. Data are shown as mean ± SD. Number of biological replicates = 3. (*D*) Western blot assays of Usp16 and ubH2A levels in control and $Usp16^{KO}$ BM. Usp16 level was quantified by ImageJ software and labeled under the ubH2A panel. GAPDH and H3 were used as loading controls. (*E*) Absolute number of erythrocytes, monocytes, granulocytes, T cells, and B cells per femur in control and $Usp16^{KO}$ mice. Data are shown as mean ± SD; $n = 6$ mice per group. Cell number was calculated as described in *Materials and Methods*. (*F*) Kaplan–Meier survival curve of control $Usp16^{+/+}$:*Mx1-Cre* and $Usp16^{2Loxp/2Loxp}$:*Mx1-Cre* mice after pIpC injection. Deletion of *Usp16* is lethal in mice.

mouse embryonic stem cells (ESCs), and differentiated ESCs (27, 28). These observations suggest that Usp16 could be the primary enzyme that antagonizes the H2A ubiquitination function of PRC1. Intriguingly, recent work in the Ts65Dn mouse model of Down's syndrome revealed that triplication of the *USP16* gene, due to trisomy of human chromosome 21, reduces HSC self-renewal, possibly contributing to the aberrant hematopoietic phenotype and elevated rates of hematopoietic disease in Down's syndrome patients (29). However, the function of this protein in normal hematopoiesis remains unknown. The results to be presented in this work suggest that triplication of *USP16* might have some bearing on the hematopoietic diseases in Down's syndrome patients.

In this study, we investigated the role of Usp16 in mouse hematopoiesis. We discovered that conditional deletion of *Usp16* in BM of 6- to 8-wk-old mice resulted in a significant increase of global ubH2A levels, consistent with a role in regulating ubH2A levels in the hematopoietic system. Furthermore, *Usp16* deletion

was associated with a dramatic reduction in mature and progenitor cell populations but did not alter HSC numbers, indicating a function in controlling embryonic and somatic stem cell lineage commitment. ChIP-seq studies revealed that the Usp16 protein bound to transcription start sites of many important genes regulating hematopoiesis. RNA-sequencing (RNA-seq) analyses showed that *Usp16* deletion resulted in altered expression of genes involved in chromatin regulation and hematopoiesis. Importantly, the altered gene expression was partially rescued by knockdown of PRC1 subunits, demonstrating that Usp16 and PRC1 coordinate to regulate ubH2A level and gene expression in the hematopoietic system. Finally, we identified *Cdkn1a* as an important downstream target of Usp16 in regulating HSC cell cycle entry and lineage commitment. In summary, these studies identify Usp16 as one of the H2A deubiquitinases that regulate ubH2A level and gene expression in the hematopoietic system and further reveal that Usp16 regulates hematopoiesis through maintaining normal HSC cell cycle profile.

Results

***Usp16* Is Required for Mouse Hematopoiesis.** Constitutive knockout of *Usp16* in mice causes embryonic lethality by preventing ESC lineage commitment (27). To determine the tissue-specific function of *Usp16*, we generated the *Usp16* conditional knockout mouse model, in which *Usp16* exons 5 and 6 are flanked with LoxP sites. The catalytic cysteine 205 residue is located in exon 6. The homozygote mice were crossed to *Mx1-cre* mice (Fig. 1*A*). Exons 5 and 6 were deleted in 6- to 8-wk-old mice by i.p. injection of polyinosinepolycytidine (pIpC). PCR-mediated genotyping of BM revealed that these two exons were efficiently deleted, as indicated by the disappearance of the predeleted allele (Fig. 1*B*, flox allele) and the concomitant appearance of the deleted allele (Fig. 1*B*, KO allele). Quantitative reverse transcription PCR (RT-qPCR) analyses revealed that *Usp16* transcript (hereafter referred as $Usp16^{KO}$) was reduced by ∼95, ∼75, and ∼85% in BM, liver, and spleen, respectively; and, as expected, the levels in heart and lung were not changed (Fig. 1*C*). The deletion of *Usp16* in BM was also confirmed at the protein level by Western blot (Fig. 1*D*, *Top* two panels; compare lanes 1 and 3 with 2 and 4). Notably, $Usp16^{KO}$ resulted in a significant increase of global ubH2A level in BM (Fig. 1*D*, *Bottom* two panels; compare lanes 1 and 3 with 2 and 4).

To determine the effect of $Usp16^{KO}$ on mouse hematopoiesis, we first analyzed peripheral blood. Complete blood count (CBC) analyses revealed a twofold reduction of red blood cells, a nearly fivefold reduction of white blood cells, and an over fivefold reduction of platelets in $Usp16^{KO}$ mice compared with control mice (Fig. S1*A*). *Usp16* deletion also caused hypo-cellularity in BM. There was an over twofold reduction of total BM cells and a nearly fourfold reduction of BM cells after red blood cell lysis (no RBC) (Fig. S1*B*). The hypo-cellularity of $Usp16^{KO}$ BM was independently confirmed by bone sections (Fig. S1*C*). This effect was specific for BM, as neither the size nor the cell number of the spleen and thymus were affected (Fig. S1*D*). Immunophenotyping of mature cell populations in BM revealed that *Usp16* deletion resulted in a significant reduction of erythrocytes, monocytes, granulocytes, and B cells; however, T-cell numbers were not altered (Fig. 1*E*; Fig. S1 *E* and *F*). Finally, mice with deletion of *Usp16* died around 2 wk after pIpC injection (Fig. 1*F*). Taken together, our data demonstrate that Usp16 regulates ubH2A levels in BM and that *Usp16* is required for mouse hematopoiesis and survival.

***Usp16* Deletion Reduces Hematopoietic Progenitor Cell Number.** The dramatic decrease in nearly all mature BM cell populations in $Usp16^{KO}$ mice suggests that Usp16 may regulate hematopoietic progenitor cell function. To investigate this possibility, we quantified progenitor cell populations in control and $Usp16^{KO}$ BM (Fig. 2). Immunophenotyping revealed that the number of common myeloid progenitors (CMP; $Lin^-Sca1^-c\text{-}Kit^+IL7R^-CD16/32^{lo}CD34^{hi}$), granulocyte monocyte progenitors (GMP; $Lin^-Sca1^-c\text{-}Kit^+IL7R^-CD16/32^{hi}CD34^{hi}$), and megakaryocyte erythroid progenitors (MEP; $Lin^-Sca1^-c\text{-}Kit^+IL7R^-CD16/32^{lo}CD34^{lo}$) was significantly reduced in $Usp16^{KO}$ BM relative to the control (Fig. 2 *A* and *B*, *Left*). The differential reduction of progenitor cell populations in $Usp16^{KO}$ BM results in a shift in the relative ratio of CMP and GMP to MEP population (Fig. 2*B*, *Right*). The number and frequency of common lymphoid progenitor (CLP; $Lin^-Sca1^{lo}c\text{-}Kit^{lo}CD127^+$) were also significantly reduced (Fig. 2 *C* and *D*). The reduction in various progenitor cell types in $Usp16^{KO}$ BM is not due to increased apoptosis. Annexin V staining revealed no significant difference in the apoptotic rate between control and $Usp16^{KO}$ BM (Fig. S2). Collectively, these observations suggest that *Usp16* may regulate the generation of these progenitor cells from HSCs.

***Usp16* Deletion Does Not Change HSC Number.** To determine how Usp16 regulates the production of progenitor cells from HSCs, we measured the effect of *Usp16* deletion on HSC cell number and frequency within the $Lin^-Sca1^+c\text{-}Kit^+$(LSK) $CD48^-CD150^+$ subsets (Fig. 3*A*). We discovered that, compared with the control, there was a fivefold increase in the frequency of LSK cell population (Fig. 3*B*, *Left*) but a 17-fold decrease of the myeloid progenitor (MyePro) cell population (Fig. 3*B*, *Right*) in $Usp16^{KO}$ BM. However, the absolute number for long-term HSC (LT-HSC; $Lin^-Sca1^+c\text{-}Kit^+CD48^-CD150^+$), short-term HSC (ST-HSC; $Lin^-Sca1^+c\text{-}Kit^+CD48^+CD150^+$), and restricted lineage progenitors (RLP; $Lin^-Sca1^+c\text{-}Kit^+CD48^+CD150^-$) did not change significantly (Fig. 3 *A* and *C*). As a consequence, there was a dramatic increase in HSC (LT-HSC, ST-HSC, and RLP) frequency after normalization to total BM cells (Fig. 3*D*). Annexin V staining revealed that *Usp16* deletion does not affect the apoptosis of LSK, LT-HSC, ST-HSC, and RLP (Fig. S3). Collectively, these data indicate that *Usp16* is required for HSC to differentiate into downstream MyePro cells whereas the transition from LT-HSC to ST-HSC and to RLP is not apparently affected by *Usp16* deletion.

***Usp16* Regulates Bone Marrow Repopulation Ability.** To determine whether *Usp16* regulates hematopoiesis in a cell-autonomous manner, we measured the colony-forming ability of $Usp16^{KO}$ BM. Clonogenic assays in the presence of IL-7, which supports the growth of B-lymphoid lineages, revealed a nearly twofold reduction in the number of pre–B-cell colonies upon *Usp16* deletion (Fig. 4*A*). The number of colony forming unit (CFU) of granulocyte and monocyte (GM), granulocyte (G), and macrophage (M) colonies was similarly reduced (Fig. 4*A*). The number of burst forming unit-erythroid (BFU-E) was also reduced, although to a lesser extent (Fig. 4*A*). Interestingly, the number of CFU of granulocyte, erythrocyte, monocyte/macrophage, megakaryocyte (GEMM) clones was not affected. These observations are consistent with the in vivo immunophenotyping of $Usp16^{KO}$ BM (Figs. 2 and 3). Serial replating assays also supported the cell-autonomous role of *Usp16* in myeloid and pre–B-colony formation (Fig. 4*B*).

To confirm the notion that *Usp16* regulates hematopoiesis, at least in part, through a cell-autonomous mechanism, we performed competitive repopulation assays. At all donor cell ratios, $Usp16^{KO}$ $CD45.2^+$ donor BM failed to repopulate either the B or the myeloid cell lineage, whereas control $CD45.2^+$ BM repopulated normally (Fig. 4*C*, *Left* and *Middle*; Fig. S4). A significant difference in T-cell repopulating ability was observed at weeks 8 and 12 posttransplantation (Fig. 4*C*, *Right*). These data reveal that Usp16 is required for the repopulating ability of all BM cell lineages. The difference between the effect of $Usp16^{KO}$ on T-cell number (Fig. 1*E*) and the requirement of Usp16 for T-cell repopulation (Fig. 4*C*) is likely due to the long lifetime of T cells. Importantly, the reduction of HSC repopulating ability even 4 wk

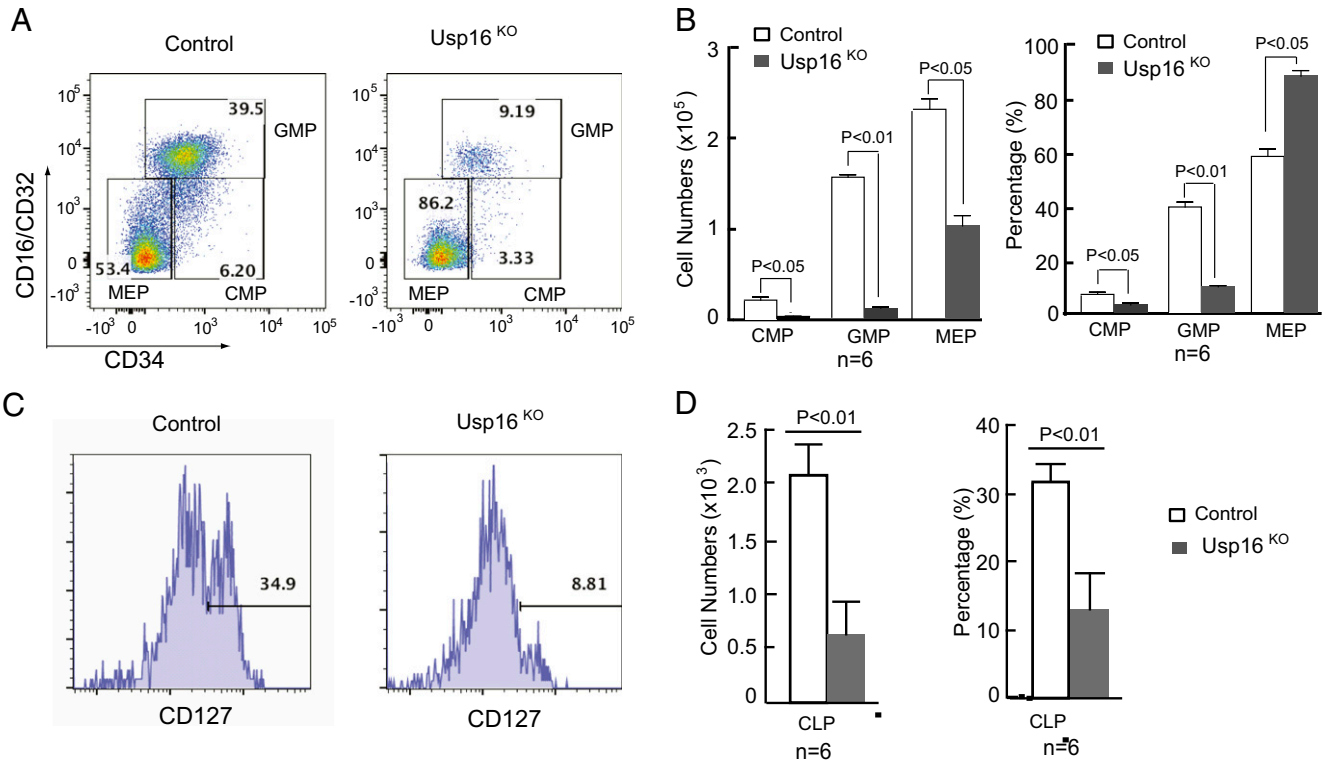

Fig. 2. *Usp16* deletion reduces hematopoietic progenitor cell number. (*A*) Representative flow cytometric profiles of CMP, GMP, and MEP populations in BM of control and $Usp16^{KO}$ mice. (*B*) Absolute number and frequency of CMP, GMP, and MEP populations per femur in control and $Usp16^{KO}$ mice. Data are shown as mean ± SD; $n = 6$ mice per group. Cell number and frequency were calculated as described in *Materials and Methods*. (*C*) Representative flow cytometric profiles of CLP populations in control and $Usp16^{KO}$ BM. (*D*) Absolute number and frequency of CLP populations per femur in control and $Usp16^{KO}$ mice. Data are shown as mean ± SD; $n = 6$ mice per group. Cell number and frequency were calculated as described in *Materials and Methods*.

posttransplantation indicates an absolute requirement for Usp16 in HSC differentiation. Alternatively, Usp16 may be required for HSC homing to BM or HSC survival after homing. The detection of residential donor BM in repopulated B-cell and myeloid lineages at a high ratio (2:1 or 4:1, 4 wk time point) and the partial repopulation of T-cell lineage at the 4:1 ratio suggested that Usp16 likely regulates HSC differentiation (Fig. 4*C*). As a direct test of this notion, we compared the homing ability of control and $Usp16^{KO}$ LSK cells (Fig. 4 *D* and *E*). Flow cytometry identification of $CD45.2^{+}$ donor cells, simultaneously identifying LSK cell populations, did not reveal any difference between control and $Usp16^{KO}$ LSK cells, supporting our conclusion that Usp16 affects mainly HSC differentiation, rather than homing of these cells.

Usp16 Regulates HSC Gene Expression in Cooperation with PRC1. To identify genes regulated by Usp16, we purified hematopoietic stem and progenitor cells (HSPCs, $Lin^{-}Sca1^{+}ckit^{+}$, LSK) and measured gene expression changes by RNA-seq in response to *Usp16* deletion (Fig. 5). *Usp16* deletion did not affect the overall transcriptome (Fig. 5*A*), but it led to differential expression of 594 genes (FPKM > 1, FPKM fold change >1.5 cutoff), with 308 genes up-regulated and 286 genes down-regulated (Fig. 5*A* and Dataset S1). Gene ontology analysis revealed that up-regulated genes are particularly enriched in categories related to cellular responses to stimulus: defense response, stress response, inflammatory response, immune response, and immune system development. Interestingly, hematopoietic or lymphoid organ development and myeloid cell differentiation were also identified as enriched categories (Fig. S5*A*). Down-regulated genes are particularly enriched for two large categories: (*i*) general biological processes including transcription regulation, chromosome organization, and regulation of kinase activity; and (*ii*) genes involved in hematopoiesis, hematopoietic or lymphoid organ development, immune system development, and leukocyte differentiation (Fig. S5*B*).

We next confirmed the RNA-seq result by measuring the expression of four randomly chosen up-regulated (*Acin 1*, *Lin28a*, *Hmga1*, and *Cdkn1a*) and nine randomly chosen down-regulated (*Rnf144b*, *Ehmt1*, *Plag1*, *Tcf3*, *Rad54i*, *Egr1*, *Cbfa2t2*, *Mirlet7i*, and *Amigo2*) genes with RT-qPCR in highly purified HSCs ($Lin^{-}Sca1^{+}c\text{-}Kit^{+}CD48^{-}CD150^{+}$) (Fig. S5*C*). Interestingly, the expression of many Usp16-bound genes appears to correlate inversely with the Bmi1-regulated gene expression reported previously (30) (Fig. 5*B*), revealing a counterbalance effect of Usp16 in PRC1 function during hematopoiesis. To test this hypothesis, we knocked down PRC1 subunits in Usp16-deleted HSCs and examined the effects on Usp16-regulated gene expression. When *Bmi1* or *Ring1B* was knocked down (Fig. S5*D*; ~21 and ~27% of the RNA transcripts remains, respectively), we observed that the expression of *Acin1* and *Cdkn1a*, which were up-regulated in $Usp16^{KO}$ HSCs, and *Rnf144b*, *Ehmt1*, *Tcf3*, and *Egr1*, which were down-regulated in $Usp16^{KO}$ HSCs, was partially restored relative to the control (Fig. 5*C*). These results support our hypothesis that Usp16 and PRC1 counterbalance each other to regulate gene expression.

To determine how Usp16 regulates gene expression, we measured the binding profile of Usp16 in HSPCs by ChIP-seq. Usp16 is enriched at the promoter/transcription start site of 2,461 genes (Fig. 5*E* and Dataset S2). These include many important hematopoietic regulators such as *Lin28a*, *HoxA9*, *HoxA7*, *HoxA10*, *Klf1/2*, *Kmt2a*, *Foxo3*, *Tbx3*, *Runx1*, *Cdkn1a*, *mTor*, *HDAC3*, *Nop10*, etc. (Fig. 5*D* and Dataset S2), suggesting that Usp16 is a potential regulator for these genes in the hematopoiesis system. Interestingly, genes bound by Usp16 showed a limited overlap with genes that exhibited significant changes in

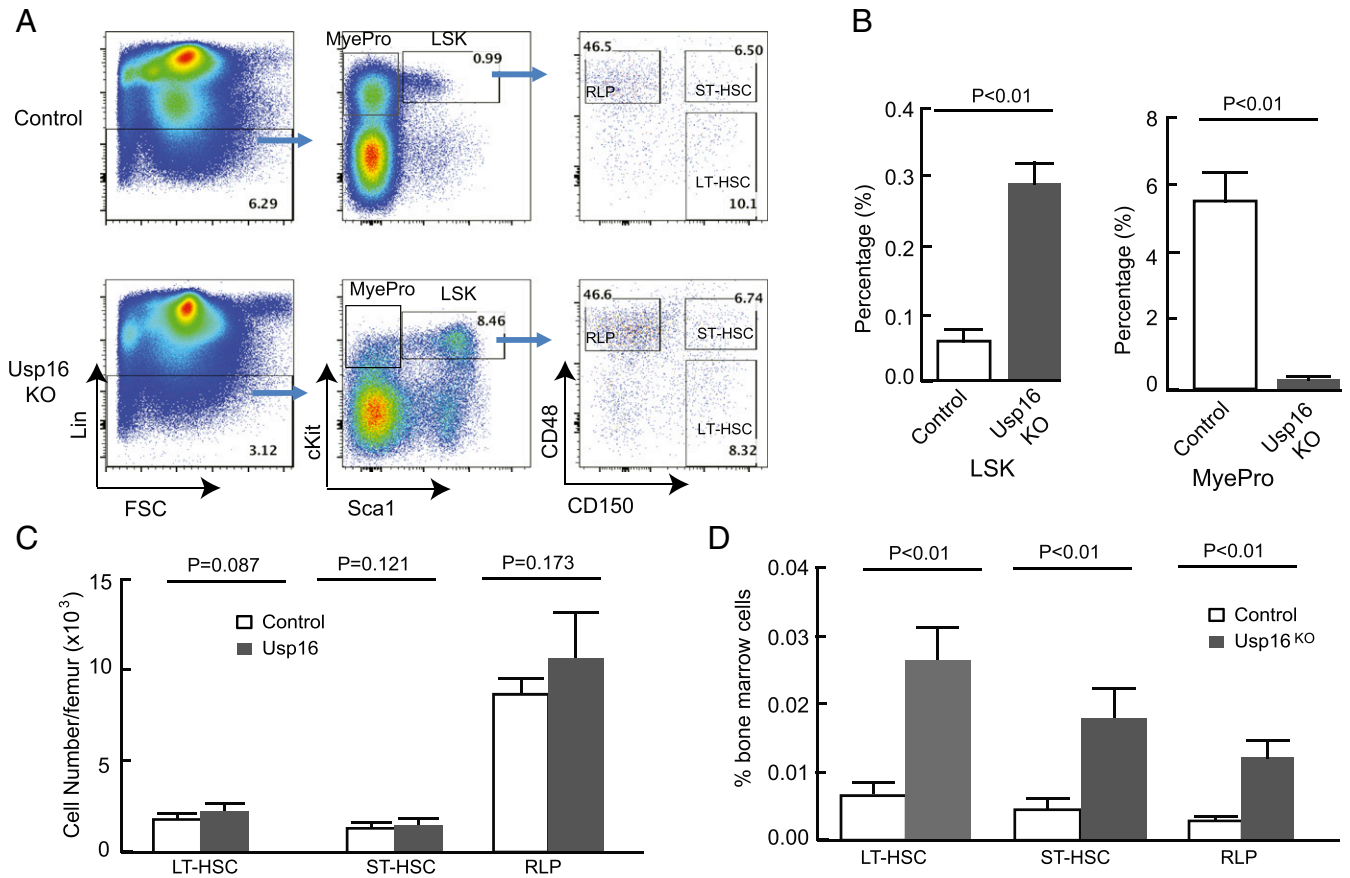

Fig. 3. *Usp16* deletion does not change HSC number. (*A*) Representative FACS plots showing analysis of HSC subsets for *Usp16*$^{+/+}$ (*Top*) and *Usp16*^{KO} (*Bottom*) BM. (*B*) Comparison of the frequencies of LSK (*Left*) and MyePro (*Right*) cells in control and *Usp16*^{KO} BM. There was a significant increase of LSK cells but a significant reduction of MyePro cell frequencies, indicating that Usp16 is required for LSK differentiation into downstream MyePro cells. Data are shown as mean ± SD; $n = 6$ mice per group. Frequency was calculated as described in *Materials and Methods*. (*C* and *D*) Comparison of the absolute cell number (*C*) and frequencies (*D*) of LT-HSC, ST-HSC, and RLP per femur in control and *Usp16*^{KO} BM. There is a significant increase of the frequency of LT-HSC, ST-HSC, and RLP in *Usp16*^{KO} BM, but the absolute cell numbers do not change. Data are shown as mean ± SD; $n = 6$ mice per group. Cell number and frequency were calculated as described in *Materials and Methods*.

response to conditional *Usp16*^{KO} (Fig. 5*E* and Dataset S3). These data indicate that Usp16 regulates the expression of many genes through an indirect mechanism, consistent with our previous study in mouse ESCs (27).

Knockdown of *p21cip1* Rescued the Differentiation Defect of *Usp16*^{KO} HSCs. Of Usp16-regulated genes, *Cdkn1a* (*p21Cip1*) is also directly bound by the Usp16 protein. The up-regulation of the *p21cip* RNA upon *Usp16* deletion was confirmed at the protein level, and interestingly, we also observed an increase of the p53 protein, which up-regulates *p21cip1* RNA transcription upon DNA damage and during quiescence (Fig. 6*A*; compare lanes 1 and 3 with 2 and 4) (31, 32). Consistent with the increased p21cip1 expression, BrdU incorporation assays revealed that the cell population in the S and G2/M phase of the cell cycle was significantly reduced in *Usp16*^{KO} HSCs whereas the population in the G0/1 phase of the cell cycle was significantly increased (Fig. 6*B* and Fig. S6*A*). The increase in G0/G1 cells was largely due to the increase in G0-phase cells, as the G1-phase cell population was significantly reduced (Fig. 6*C* and Fig. S6*B*). These studies revealed that *Usp16* deletion disturbed the cell cycle status of HSCs, resulting in a higher population of quiescent HSCs.

As it has been proposed that stem cells receive differentiation signals during the G1 phase of the cell cycle (33, 34), the reduction in G1-phase cell populations could explain the undifferentiated phenotype of *Usp16*^{KO} HSCs (Fig. 3). To explore this possibility, we knocked down p21cip1 in *Usp16*^{KO} HSCs and examined the effect on HSC differentiation. When p21cip1 was knocked down to a level similar to that in control HSCs, the p53 level was not affected (Fig. 6*D*). Nevertheless, p21cip1 knockdown largely restored the differentiated phenotype of *Usp16*^{KO} HSCs. The numbers of CFU-G, CFU-M, and CFU-GM from *Usp16*^{KO} HSCs were increased to close to the numbers derived from control HSCs (Fig. 6*E*). The number of BFU-E was also increased, although the increase was not statistically significant (Fig. 6*E*). Consistent with our in vitro colony formation assay, CFU-GEMM number did not change significantly (Fig. 6*E*). The rescue of the differentiation defects of *Usp16*^{KO} HSCs by p21cip1 was also observed in vivo. As shown in Fig. 6*F* and Fig. S6*C*, *Usp16*^{KO} completely abolished the differentiation of CD45.2^{+} HSCs to downstream MyePro cells; however, knockdown of p21cip1 in *Usp16*^{KO} HSCs largely restored the differentiation ability. Interestingly, we did not detect mature hematopoietic cell lineages in peripheral blood from rescued HSPCs after p21cip knockdown (Fig. S6*D*), suggesting that Usp16 is also required for downstream cell lineage commitment. Taken together, these data suggest that cell cycle regulation by p21cip1 is largely responsible for the effect of *Usp16* deletion on hematopoiesis and HSC differentiation.

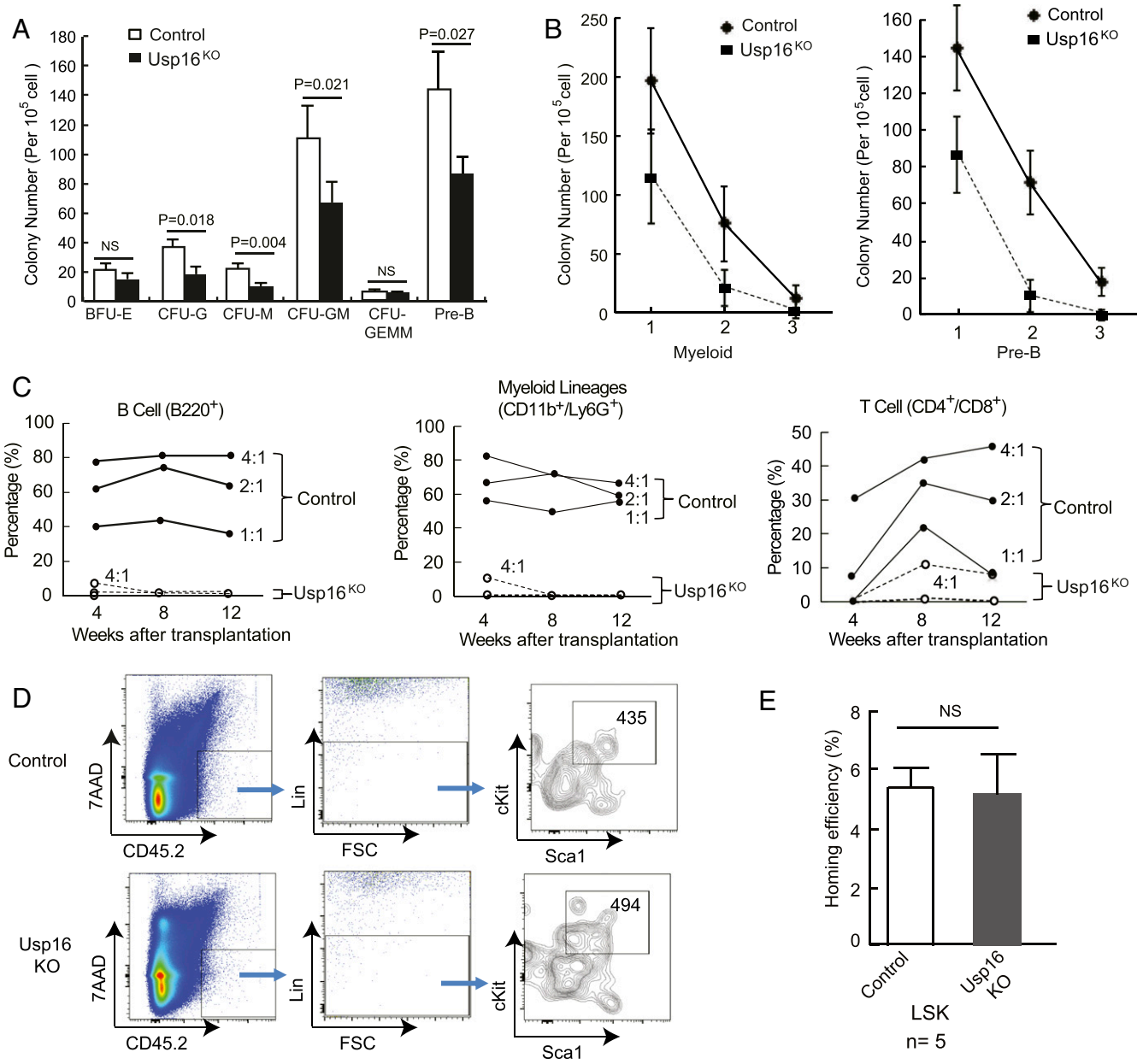

Fig. 4. Usp16 regulates hematopoiesis cell-autonomously. (*A*) Colony-forming assay of control and *Usp16*^{KO} BM. BM cells were isolated from control and *Usp16*^{KO} mice and mixed with methycellulose (M03434 and M03630, StemCell Technologies). Colony number was examined after 7–10 d (M03630) or 10–12 d (M03434). (*B*) Serial replating assay of control and *Usp16*^{KO} BM. (*C*) Percentage of test (CD45.2) versus competitor (CD45.1) cells at different time points posttransplantation. (*D*) Homing assay of control and *Usp16*^{KO} LSK cells. Representative flow cytometric profiles for gating CD45.2^{+} LSK cells are shown. (*E*) Homing efficiency for control and *Usp16*^{KO} LSK cells.

Discussion

Hematopoiesis in vivo is driven by developmental stage-specific transcription factors (35). As transcription factors function in a chromatin environment, their activities, and hence hematopoiesis, are profoundly affected by regulators of chromatin conformation and DNA accessibility (3). In this study, we created a conditional knockout model in the mouse hematopoietic system to examine the function of Usp16. *Usp16* knockout leads to elevated ubH2A level and hypo-cellular BM, similar to *Bmi1* and *Ring1B* knockout, indicating that the relative levels of Usp16 and PRC1 are important for optimal cellular ubH2A level and proper gene expression profiles to preserve homeostasis during hematopoiesis (Figs. 1 and 2; Fig. S1) (18, 21). Specifically, *Usp16* deletion results in a significant reduction of mature and progenitor cells but does not alter HSC numbers (Figs. 1–3), pointing to a key role of Usp16 in controlling HSC differentiation. ChIP-seq and RNA-seq analyses in highly purified HSPCs revealed that Usp16 binds to many genes important for hematopoiesis and that Usp16 deletion is associated with altered expression of genes involved in hematopoietic and lymphoid organ development and myeloid cell and leukocyte differentiation, among others (Fig. 5). The observed changes in gene expression are consistent with the defective colony formation ability in vitro and defective differentiation potential of *Usp16*^{KO} HSCs in vivo (Figs. 3 and 4).

Importantly, we found that *Usp16* deletion leads to increased p21cip1 at the RNA and protein levels, as well as to an increase of p53, the tumor suppressor protein that up-regulates *p21cip1*

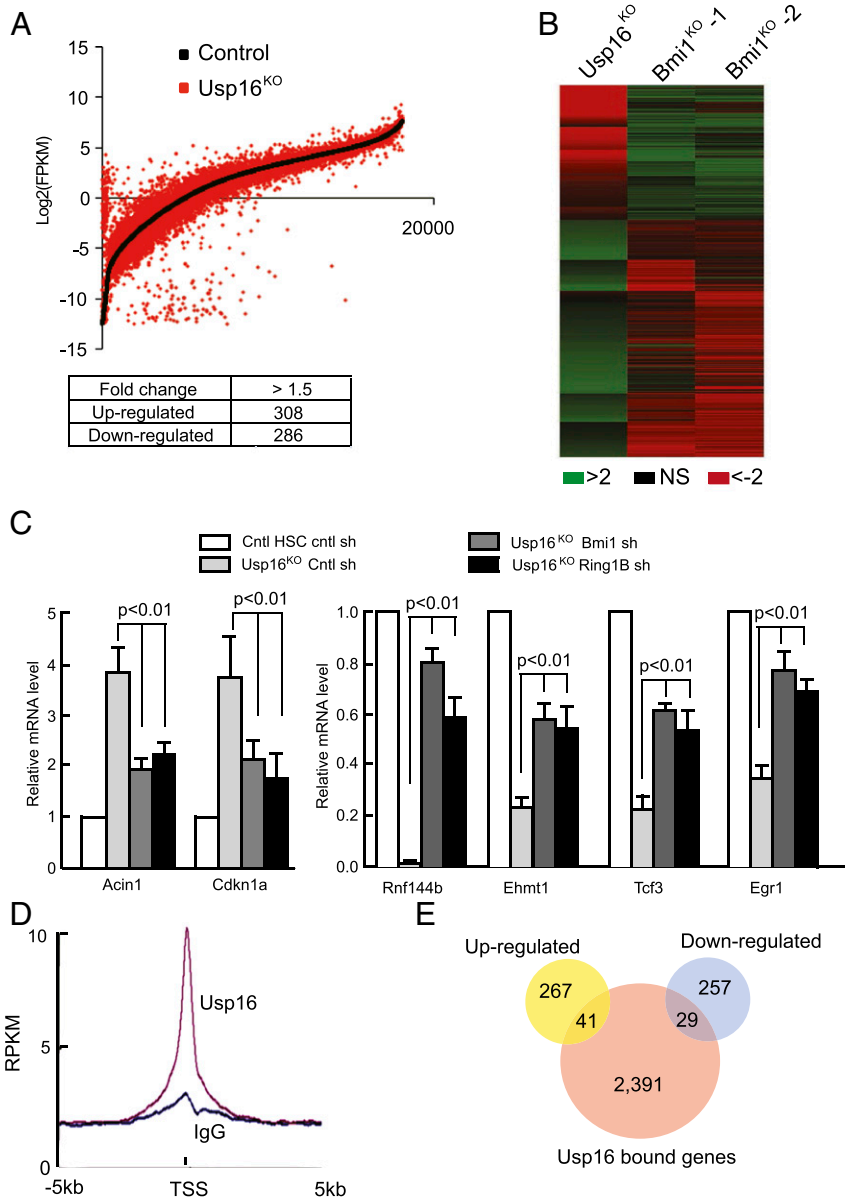

Fig. 5. Usp16 regulates gene expression in coordination with PRC1. (*A*) Scatter plot of gene expression levels in control and *Usp16*^{KO} HSPCs as determined by RNA-seq. Genes significantly dysregulated [Log_2(Fold change) > 1.5] are shown in the bottom table. (*B*) Heatmaps of the expression of Usp16-bound genes in *Usp16*- and *Bmi1*-knockout HSPCs. Gene expression regulated by Usp16 and Bmi1 is inversely correlated. Bmi1 knockout data are taken from previous publications (30). (*C*) Effects of *Bmi1* and *Ring1B* knockdown on the expression of genes that were up-regulated (*Left*) and down-regulated (*Right*) in *Usp16*^{KO} HSCs. Levels in control HSCs treated with control shRNA were arbitrarily set as 1. Data are shown as mean ± SD. Number of biological replicates = 2. (*D*) Binding profiles of Usp16 (red line) and IgG (black line) in HSPCs. Transcription start site (TSS) and regions 5 kb upstream and 5 kb downstream are shown. (*E*) Venn diagram showing genes bound by Usp16 and genes the expression of which was altered by *Usp16*^{KO} in HSPCs. Gene numbers are labeled inside each of the circles.

expression upon DNA damage (Fig. 6) (31, 32). Both p21 and p53 have been implicated in the maintenance of HSC quiescence (36, 37). Therefore, the increased p21cip1 level would explain the increase of G0 population in HSCs, which are unable to differentiate (Fig. 6). Also interesting is that our RNA-seq studies did not reveal a change in the expression of *Cdkn1b* (p27Kip1), which is a p21cip1-related inhibitor of S-phase entry into normal cycling cells. It appears that p21cip1 has a specific role in HSCs. It is worth noting that p21cip1 was originally identified in quiescent cells that also harbor high levels of p53 protein (31, 32). Consistent with its critical role in controlling hematopoiesis, p21cip1 knockdown in *Usp16*-deleted HSCs restored its differentiation potential (Fig. 6 and Fig. S6).

Because Usp16 also regulates the expression of many additional genes involved in hematopoiesis (Fig. 5), one important question is: do these genes also contribute to the undifferentiated phenotypes of *Usp16*^{KO} HSCs? If they do, what are their relationships to p21cip1 during HSC differentiation? Our data suggest that primarily the G1 phase of the cell cycle provides the critical window for HSCs to respond to developmental signals and activate these other hematopoietic regulators. When most HSCs are in the G0 phase due to elevated *Usp16*^{KO}-induced p21cip1, HSCs do not respond to the development signals and these hematopoietic regulators cannot be activated. However, many hematopoietic genes are direct targets of Usp16 (Fig. 5*D* and Dataset S2). How can this latter group of genes be activated if their ubH2A marks are not erased in *Usp16*^{KO} HSCs

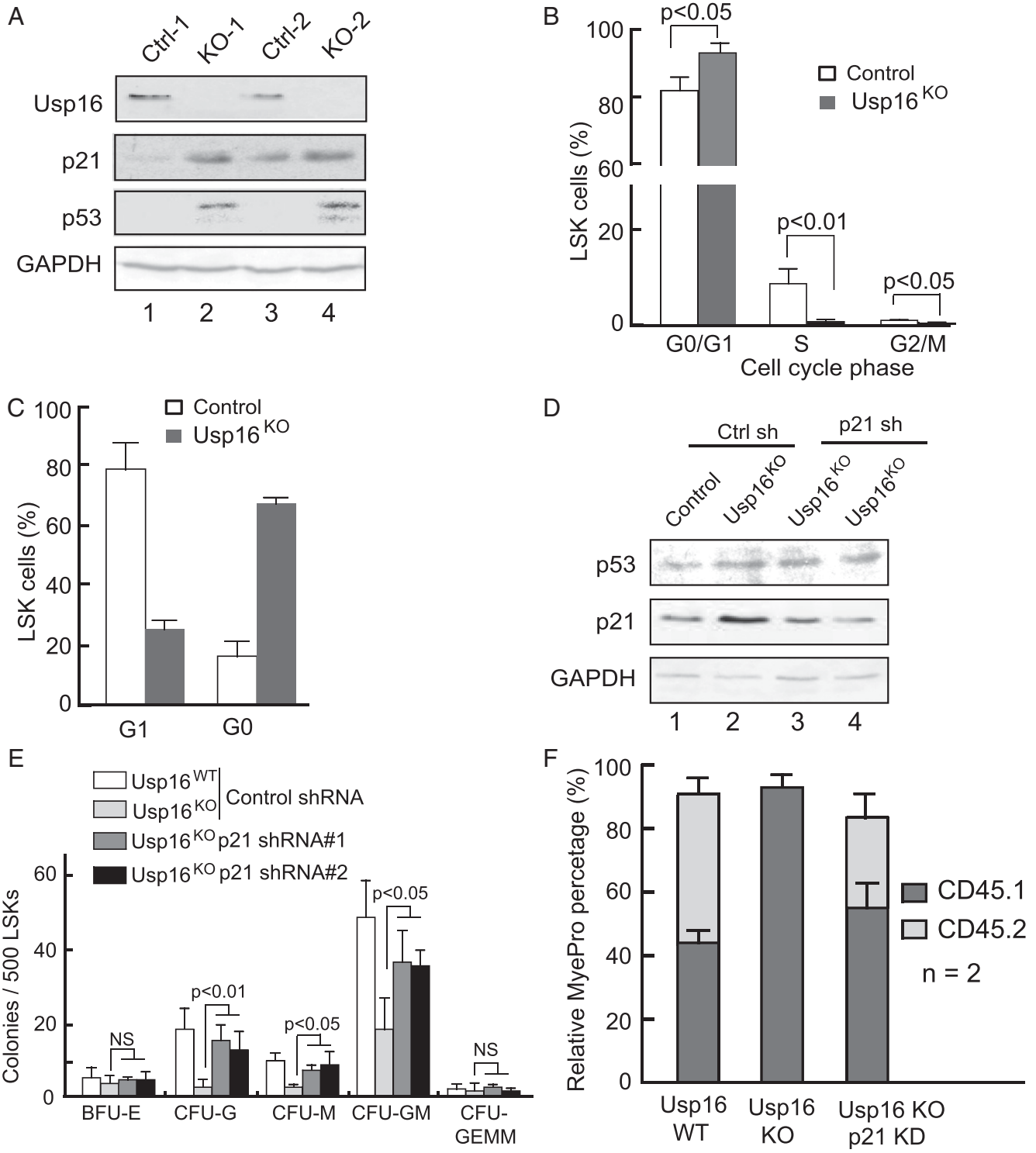

Fig. 6. Usp16 regulates HSC cycling and differentiation. (*A*) Western blot assay of p53 and p21 levels in control and *Usp16*^{KO} HSPCs. Two independent sample preparations were used. (*B*) Cell cycle distribution of control and *Usp16*^{KO} HSPCs. (*C*) Relative percentage of G0/G1 phase of control and *Usp16*^{KO} HSPCs. (*D*) Western blot assay of HSPCs from control and *Usp16*^{KO} mice infected with control shRNA or shRNA against p21cip1. (*E*) Colony formation assay of HSPCs from control and *Usp16*^{KO} mice infected with control shRNA or shRNA against p21cip1. (*F*) Relative percentage of MyePro cells derived from donor LSK cells (CD45.2^{+}) and competitor BM cells (CD45.1^{+}) in BM of recipient mice.

rescued by p21 knockdown? There are several possibilities that are not mutually exclusive. First, another H2A deubiquitinase (for example, *Mysm1*; see below) may function to eliminate these ubH2A marks. Second, the activating signals repeatedly received by HSCs during the G1 phase of the cell cycle could block the deposition of ubH2A marks by PRC1. Third, the activating signals received by HSCs during the G1 phase could override the ubH2A repressive marks and drive the expression of these hematopoietic regulators and HSC differentiation. Although further dissecting these possibilities is beyond the scope of current paper, our study highlights

the critical role of cell cycle regulation in controlling stem cell pluripotency and differentiation not only in ESCs but also in somatic stem cells (33, 34).

A reduction of mature and progenitor cells was also observed in *Mysm1* and *Usp3* knockout mice (23, 25). *Usp3* deletion reduced HSC pools due to cell cycle restriction (25). This was attributed to a defective damaged DNA repair response and unresolved spontaneous DNA damage (25) and thus different from the dysregulation of gene expression as we have described for $Usp16^{KO}$. In *Mysm1* knockout mice, there is a loss of quiescence for HSC, and hence reduced HSC numbers, impaired HSC self-renewal and differentiation, as well as increased apoptosis in progenitor cells. Together, these effects account for the final reduction of mature and progenitor cells (23, 38). In contrast, $Usp16^{KO}$ increases HSC quiescence (Fig. 6); whereas the HSC numbers and apoptosis of progenitor cells are not affected, differentiation into different lineages is impaired (Figs. 2–4; Figs. S2 and S3). Because *Mysm1* knockout does not affect the global ubH2A level, Mysm1 may control hematopoiesis (B-cell development, CLP fate determination, and natural killer cell maturation) by targeting a limited number of genes (23, 24, 39, 40). Increased reactive oxygen species, γ-H2AX foci, and p53 level were observed in $Mysm1^{KO}$ HSCs (23). Interestingly, p53 knockout fully rescues the hematopoietic defects of $Mysm1^{KO}$ HSCs (41). Compared with the complex process regulating HSC function in $Mysm1^{KO}$ mice, the undifferentiated phenotype of $Usp16^{KO}$ HSCs was largely attributable to p21cip1-regulated cell cycle entry from G0 to G1. It will be intriguing to determine the unique as well as overlapping function of Mysm1 and Usp16 in regulating hematopoiesis and hematopoietic stem cell function.

Materials and Methods

***Usp16* Hematopoietic System Deletion.** *Usp16* conditional knockout mice were described previously (27). These mice were backcrossed to the C57BL/6 genetic background for eight generations. The *Usp16* conditional knockout mice were then crossed with *Mx1-Cre* mice to obtain $Usp16^{2Lloxp/2Loxp}$*:Mx1-Cre* mice. Usp16 was deleted in 6- to 8-wk-old mice by i.p. injection of pIpC (Invivogen; 25 μg per gram of body mass) every other day for 8 d. $Usp16^{+/+}$*:Mx1-Cre* mice were injected in parallel as controls. Genotyping was conducted with PCR using primers in *SI Materials and Methods*. All animal experiments were carried out according to the guidelines for the care and use of laboratory animals of the University of Alabama at Birmingham under an Institutional Animal Care and Use Committee-approved protocol.

Flow Cytometry. For HSC staining, BM cells were incubated with the following PE-conjugated lineage marker antibodies: Ter119 (TER119), B220 (RA3-6B2), Gr-1 (1A8), CD11b (M1/17), CD3e (145-2C11), CD4 (RM4-5), CD8a (53-6.7), CD5 (53-7.3), APC-conjugated c-Kit (2B8), V500-conjugated Sca-1 (D7), PE-CY7-conjugated CD150 (mShad150), and APC-CY7-conjugated CD48 (HM48-1) antibodies. For CMP, GMP, and MEP staining, cells were incubated with PE-conjugated lineage marker antibodies, PE-CY7-conjugated c-Kit (2B8), V500-conjugated Sca-1 (D7), V450-conjugated IL7R (SB/199), FITC-conjugated CD34 (RAM34), and APC-conjugated CD16/32 (2.4G2) antibodies. For CLP staining, cells were incubated with PE-conjugated lineage marker antibodies, APC-conjugated c-Kit (2B8), V500-conjugated Sca-1 (D7), and V450-conjugated IL7R (SB/199) antibodies. Erythrocytes, monocytes, granulocytes, T cells, and B cells in peripheral blood and BM were defined as being positive for Ter119, CD11b, Ly6G, CD4/CD8, and CD19, respectively. Dead cells were excluded by staining with 7-amino actinomycin D (BD Pharmingen). After washing, labeled cells were run on BD LSR II for analysis or on BD FACSAria for sorting. The frequency of each population was calculated with the cell number of the specific population divided by the number of total BM cells within one femur. The absolute number of cells in each population was calculated by the relative percentage (derived from FACS) times the total BM cell number within one femur. CD150 antibodies were purchased from eBioscience. All other antibodies were obtained from BD Pharmingen.

Colony Formation Assay. BM was isolated from control and $Usp16^{KO}$ mice and washed with PBS once. Red blood cells were lysed by incubating with ACK buffer (150 mM NH_4Cl, 10 nM $KHCO_3$, 1 nM Na_4EDTA, pH 7.2) for 2 min. HSCs were purified as described above. BM was mixed with Methocult media 03434 and 03630 (StemCell Technologies) at a final cell density of 2×10^5 and 5×10^5 cell/mL, respectively. HSCs were mixed with Methocult media at a final concentration of 500 cells/mL. Cells were seeded onto a 35-mm dish in triplicate. BFU-E colonies were counted on days 7–10, and other colonies were counted on days 10–12.

Competitive Repopulation, Homing, and Rescue Assays. BM was isolated from control and $Usp16^{KO}$ mice. Donor BM cells ($CD45.2^+$) were mixed with 5×10^5 competitor BM cells ($CD45.1^+$) at a 1:1, 2:1, or 4:1 ratio and injected into lethally irradiated (10 Gy) recipient mice through the tail vein. Mice were maintained in neomycin (1.1 mg/L) and polymyxin B (10^6 u/L)-containing drinking water for 2 wk, and peripheral blood chimerism was analyzed at 4, 8, and 12 wk after transplantation. B-cell, T-cell, and myeloid lineages were defined as being positive for $B220^+$, $CD4^+/CD8^+$, and $CD11b^+/Ly6G^+$, respectively. Donor contribution was measured by cell surface CD45.1 and CD45.2 markers. For homing assay, 1×10^4 donor LSK cells ($CD45.2^+$) from control and $Usp16^{KO}$ mice were transplanted into irradiated (4.5 Gy) recipient mice ($CD45.1^+$). $CD45.2^+$ LSK cells in recipient BM were quantified after 16 h. Homing efficiency was calculated by dividing the number of $CD45.2^+$ LSK cells in BM of recipient mice with total injected LSK cells (1×10^4 cells). For rescue experiment, LSK cells were isolated from control and $Usp16^{KO}$ mice ($CD45.2^+$) and transduced with p21cip1 shRNAs. A total of 2,000 transduced LSK cells were then mixed with 3×10^5 competitor bone marrow cells ($CD45.1^+$) and injected into lethally irradiated CD45.1 mice. Relative contribution to MyePro cells from donor LSK cells and competitor bone marrow were determined 7 d after transplantation. Relative contribution to B cells and myeloid lineage from donor LSK cells and competitor bone marrow were determined 5 wk after transplantation.

shRNA Knockdown. Control and shRNAs against p21cip1 were obtained from Addgene (42). These lentiviral constructs were transfected into 293T cells together with pCMVd8.91 and pvsv.g. Targeting sequences for *Bmi1* (ACAACCAGAATCAAGATCA) and *Ring1B* (ACGGAACTCAACCATTAAG) were cloned into pLKO.1 vector. Viruses were generated in 293T cells with calcium phosphate transfection. Virus-containing media were collected, filtered, and concentrated by ultracentrifugation. HSCs (2×10^4) were infected in the presence of polybrene in DMEM, 10% (vol/vol) FBS, stem cell factor (50 ng/mL), and interleukin 6 (5 ng/mL). Control and p21cip1 shRNA infected HSCs were purified with GFP expression through FACS sorting. Control and Bmi1 and Ring1B shRNA-infected HSCs were selected with puromycin (5 μg/mL) for 36 h.

Cell Cycle and Apoptosis Analysis. Mice were injected with 3 mg BrdU (in PBS) intraperitoneally 3 h before BM isolation. BrdU incorporation was analyzed using the FITC BrdU Flow Kit (BD, 51–2354ak) following the manufacturer's protocol. G1 and G0 cell populations were distinguished using Hoechst 33342 (Molecular Probe, H3570) and Pyronin Y (Sigma, P9172-1G) staining. Briefly, BM cells were resuspended at a concentration 10^6 cells/mL with PBS buffer containing 2% (vol/vol) FBS and 10 μM Hoechst 33342 and incubated at 37 °C for 30 min. Cells were then washed with PBS containing 20 mM Hepes, 1 mg/mL glucose, 10% (vol/vol) FBS, 10 μM Hoechst 33342, and 1 μg/mL Pyronin Y; resuspended at a concentration 5×10^6 cells/mL in the same buffer; and incubated at 37 °C for 30 min. Cells were washed twice with PBS and incubated with surface marker antibodies for LSK cells as described above. Dead cells and cell aggregate were excluded from cell cycle analysis. Apoptosis was analyzed using FITC Annexin V Apoptosis Detection Kit (BD, 556547) following the manufacturer's instruction.

ChIP-seq, RNA-seq, and RT-qPCR experiments and data analyses are presented as *SI Materials and Methods*. The RNA-seq and ChIP-seq data have been deposited in the Gene Expression Omnibus (GEO) under accession no. GSE62825.

ACKNOWLEDGMENTS. We thank Mr. M. Spell at the University of Alabama at Birmingham Flow Cytometry Core for assistance with FACS analyses. H.W. is a Leukemia and Lymphoma Scholar and is supported by NIH Grant GM081489.

1. Rice KL, Hormaeche I, Licht JD (2007) Epigenetic regulation of normal and malignant hematopoiesis. *Oncogene* 26(47):6697–6714.
2. Sashida G, Iwama A (2012) Epigenetic regulation of hematopoiesis. *Int J Hematol* 96(4):405–412.
3. Cullen SM, Mayle A, Rossi L, Goodell MA (2014) Hematopoietic stem cell development: An epigenetic journey. *Curr Top Dev Biol* 107:39–75.
4. Margueron R, Reinberg D (2011) The Polycomb complex PRC2 and its mark in life. *Nature* 469(7330):343–349.

5. Prezioso C, Orlando V (2011) Polycomb proteins in mammalian cell differentiation and plasticity. *FEBS Lett* 585(13):2067–2077.
6. Surface LE, Thornton SR, Boyer LA (2010) Polycomb group proteins set the stage for early lineage commitment. *Cell Stem Cell* 7(3):288–298.
7. Levine SS, et al. (2002) The core of the polycomb repressive complex is compositionally and functionally conserved in flies and humans. *Mol Cell Biol* 22(17):6070–6078.
8. Wang H, et al. (2004) Role of histone H2A ubiquitination in Polycomb silencing. *Nature* 431(7010):873–878.
9. de Napoles M, et al. (2004) Polycomb group proteins Ring1A/B link ubiquitylation of histone H2A to heritable gene silencing and X inactivation. *Dev Cell* 7(5):663–676.
10. Wei J, Zhai L, Xu J, Wang H (2006) Role of Bmi1 in H2A ubiquitylation and Hox gene silencing. *J Biol Chem* 281(32):22537–22544.
11. Buchwald G, et al. (2006) Structure and E3-ligase activity of the Ring-Ring complex of polycomb proteins Bmi1 and Ring1b. *EMBO J* 25(11):2465–2474.
12. Cao R, Tsukada Y, Zhang Y (2005) Role of Bmi-1 and Ring1A in H2A ubiquitylation and Hox gene silencing. *Mol Cell* 20(6):845–854.
13. Zhou W, et al. (2008) Histone H2A monoubiquitination represses transcription by inhibiting RNA polymerase II transcriptional elongation. *Mol Cell* 29(1):69–80.
14. Stock JK, et al. (2007) Ring1-mediated ubiquitination of H2A restrains poised RNA polymerase II at bivalent genes in mouse ES cells. *Nat Cell Biol* 9(12):1428–1435.
15. Martin-Perez D, Piris MA, Sanchez-Beato M (2010) Polycomb proteins in hematologic malignancies. *Blood* 116(25):5465–5475.
16. Iwama A, Oguro H, Negishi M, Kato Y, Nakauchia H (2005) Epigenetic regulation of hematopoietic stem cell self-renewal by polycomb group genes. *Int J Hematol* 81(4): 294–300.
17. Sauvageau M, Sauvageau G (2010) Polycomb group proteins: Multi-faceted regulators of somatic stem cells and cancer. *Cell Stem Cell* 7(3):299–313.
18. van der Lugt NM, et al. (1994) Posterior transformation, neurological abnormalities, and severe hematopoietic defects in mice with a targeted deletion of the bmi-1 proto-oncogene. *Genes Dev* 8(7):757–769.
19. Park IK, et al. (2003) Bmi-1 is required for maintenance of adult self-renewing haematopoietic stem cells. *Nature* 423(6937):302–305.
20. Lessard J, Sauvageau G (2003) Bmi-1 determines the proliferative capacity of normal and leukaemic stem cells. *Nature* 423(6937):255–260.
21. Calés C, et al. (2008) Inactivation of the polycomb group protein Ring1B unveils an antiproliferative role in hematopoietic cell expansion and cooperation with tumorigenesis associated with Ink4a deletion. *Mol Cell Biol* 28(3):1018–1028.
22. Cao J, Yan Q (2012) Histone ubiquitination and deubiquitination in transcription, DNA damage response, and cancer. *Front Oncol* 2:26.
23. Nijnik A, et al.; Sanger Institute Microarray Facility; Sanger Mouse Genetics Project (2012) The critical role of histone H2A-deubiquitinase Mysm1 in hematopoiesis and lymphocyte differentiation. *Blood* 119(6):1370–1379.
24. Jiang XX, et al. (2011) Control of B cell development by the histone H2A deubiquitinase MYSM1. *Immunity* 35(6):883–896.
25. Lancini C, et al. (2014) Tight regulation of ubiquitin-mediated DNA damage response by USP3 preserves the functional integrity of hematopoietic stem cells. *J Exp Med* 211(9):1759–1777.
26. Nicassio F, et al. (2007) Human USP3 is a chromatin modifier required for S phase progression and genome stability. *Curr Biol* 17(22):1972–1977.
27. Yang W, et al. (2014) The histone H2A deubiquitinase Usp16 regulates embryonic stem cell gene expression and lineage commitment. *Nat Commun* 5:3818.
28. Joo HY, et al. (2007) Regulation of cell cycle progression and gene expression by H2A deubiquitination. *Nature* 449(7165):1068–1072.
29. Adorno M, et al. (2013) Usp16 contributes to somatic stem-cell defects in Down's syndrome. *Nature* 501(7467):380–384.
30. Oguro H, et al. (2010) Poised lineage specification in multipotential hematopoietic stem and progenitor cells by the polycomb protein Bmi1. *Cell Stem Cell* 6(3):279–286.
31. Besson A, Dowdy SF, Roberts JM (2008) CDK inhibitors: Cell cycle regulators and beyond. *Dev Cell* 14(2):159–169.
32. Duronio RJ, Xiong Y (2013) Signaling pathways that control cell proliferation. *Cold Spring Harb Perspect Biol* 5(3):a008904.
33. Vallier L (2015) Cell cycle rules pluripotency. *Cell Stem Cell* 17(2):131–132.
34. Singh AM, Dalton S (2009) The cell cycle and Myc intersect with mechanisms that regulate pluripotency and reprogramming. *Cell Stem Cell* 5(2):141–149.
35. Mercer EM, Lin YC, Murre C (2011) Factors and networks that underpin early hematopoiesis. *Semin Immunol* 23(5):317–325.
36. Cheng T, et al. (2000) Hematopoietic stem cell quiescence maintained by p21cip1/waf1. *Science* 287(5459):1804–1808.
37. Liu Y, et al. (2009) p53 regulates hematopoietic stem cell quiescence. *Cell Stem Cell* 4(1):37–48.
38. Wang T, et al. (2013) The control of hematopoietic stem cell maintenance, self-renewal, and differentiation by Mysm1-mediated epigenetic regulation. *Blood* 122(16):2812–2822.
39. Won H, et al. (2014) Epigenetic control of dendritic cell development and fate determination of common myeloid progenitor by Mysm1. *Blood* 124(17):2647–2656.
40. Nandakumar V, Chou Y, Zang L, Huang XF, Chen SY (2013) Epigenetic control of natural killer cell maturation by histone H2A deubiquitinase, MYSM1. *Proc Natl Acad Sci USA* 110(41):E3927–E3936.
41. Belle JI, et al. (2015) p53 mediates loss of hematopoietic stem cell function and lymphopenia in Mysm1 deficiency. *Blood* 125(15):2344–2348.
42. Fasano CA, et al. (2007) shRNA knockdown of Bmi-1 reveals a critical role for p21-Rb pathway in NSC self-renewal during development. *Cell Stem Cell* 1(1):87–99.
43. Langmead B, Trapnell C, Pop M, Salzberg SL (2009) Ultrafast and memory-efficient alignment of short DNA sequences to the human genome. *Genome Biol* 10(3):R25.
44. Li H, et al.; 1000 Genome Project Data Processing Subgroup (2009) The Sequence Alignment/Map format and SAMtools. *Bioinformatics* 25(16):2078–2079.
45. Zhang Y, et al. (2008) Model-based analysis of ChIP-Seq (MACS). *Genome Biol* 9(9): R137.
46. Quinlan AR, Hall IM (2010) BEDTools: A flexible suite of utilities for comparing genomic features. *Bioinformatics* 26(6):841–842.
47. Trapnell C, et al. (2010) Transcript assembly and quantification by RNA-Seq reveals unannotated transcripts and isoform switching during cell differentiation. *Nat Biotechnol* 28(5):511–515.
48. Livak KJ, Schmittgen TD (2001) Analysis of relative gene expression data using real-time quantitative PCR and the 2(-Δ Δ C(T)) method. *Methods* 25(4):402–408.